

Genes required for axon pathfinding and extension in the *C. elegans* nerve ring

Jennifer A. Zallen, Susan A. Kirch and Cornelia I. Bargmann*

Programs in Developmental Biology, Neuroscience and Genetics, Howard Hughes Medical Institute, Department of Anatomy, University of California, San Francisco, California 94143-0452, USA

*Author for correspondence (e-mail: cori@itsa.ucsf.edu)

Accepted 31 May; published on WWW 19 July 1999

SUMMARY

Over half of the neurons in *Caenorhabditis elegans* send axons to the nerve ring, a large neuropil in the head of the animal. Genetic screens in animals that express the green fluorescent protein in a subset of sensory neurons identified eight new *sax* genes that affect the morphology of nerve ring axons. *sax-3/robo* mutations disrupt axon guidance in the nerve ring, while *sax-5*, *sax-9* and *unc-44* disrupt both axon guidance and axon extension. Axon extension and guidance proceed normally in *sax-1*, *sax-2*, *sax-6*, *sax-7* and *sax-8* mutants, but these animals exhibit later defects in the maintenance of nerve ring structure. The functions of existing guidance genes in nerve ring development were

also examined, revealing that SAX-3/Robo acts in parallel to the VAB-1/Eph receptor and the UNC-6/netrin, UNC-40/DCC guidance systems for ventral guidance of axons in the amphid commissure, a major route of axon entry into the nerve ring. In addition, SAX-3/Robo and the VAB-1/Eph receptor both function to prevent aberrant axon crossing at the ventral midline. Together, these genes define pathways required for axon growth, guidance and maintenance during nervous system development.

Key words: SAX-3/Robo, VAB-1/Eph receptor, UNC-6/netrin, UNC-40/DCC, Axon growth, Guidance, *Caenorhabditis elegans*

INTRODUCTION

During development, neurons project axons that often travel long distances through diverse environments to contact their targets (Tessier-Lavigne and Goodman, 1996; Mueller, 1999). The nematode *C. elegans* provides a simple and well-characterized organism in which to study axon development. There are 302 neurons in the adult hermaphrodite, and the stereotyped position of each neuron, its processes and its putative synaptic connections are known from serial section electron micrographs (White et al., 1986). 180 of these neurons project axons into the nerve ring, the largest axon bundle in the animal. These axons must navigate to the nerve ring, recognize and enter the nerve ring, make specific contacts with each other and maintain these contacts during growth. Little is known about the genes that control nerve ring development.

Several conserved classes of guidance molecules direct axon guidance in *C. elegans* and other organisms. The UNC-6/netrin diffusible guidance cue is required for axon guidance along the dorsal-ventral axis in *C. elegans*, *Drosophila* and vertebrates (reviewed in Tessier-Lavigne and Goodman, 1996 and Culotti and Merz, 1998). Netrins attract or repel different subsets of axons in vivo and in vitro. Attraction to netrins is mediated by UNC-40/DCC, an immunoglobulin superfamily member that is thought to act as a netrin receptor on growing axons, while repulsion from netrins is mediated by UNC-5, a transmembrane receptor that acts in combination with UNC-40/DCC. UNC-6 is present in the region of the nerve ring

(Wadsworth et al., 1996), and both the UNC-40 and UNC-5 receptors are expressed in nerve ring neurons (Leung-Hagesteijn et al., 1992; Chan et al., 1996), but it is not known whether these molecules influence nerve ring axon guidance.

Nerve ring neurons also express SAX-3/Robo, a transmembrane protein in the immunoglobulin superfamily that is related to *Drosophila* and vertebrate Roundabout (Robo) proteins. Disruption of Robo function in *Drosophila* and *C. elegans* leads to inappropriate axon crossing of the ventral midline (Kidd et al., 1998; Zallen et al., 1998). *sax-3* mutants are also defective in the ventral guidance of motor and interneuron axons to the midline, suggesting a role for SAX-3/Robo in multiple guidance events (Zallen et al., 1998).

A third guidance molecule expressed in the *C. elegans* nerve ring is the VAB-1 Eph receptor tyrosine kinase (George et al., 1998). Eph receptors recognize transmembrane or GPI-linked ephrin ligands, which have been implicated primarily in repulsion of growing axons, though they may have attractive properties as well (reviewed in Flanagan and Vanderhaeghen, 1998 and Holder and Klein, 1999). The VAB-1 Eph receptor is required for normal epithelial cell migrations in *C. elegans* (George et al., 1998), but its role in axon guidance has not been described.

We initiated a genetic analysis of axon guidance in the *C. elegans* nerve ring by focusing on a subset of nerve ring sensory neurons. The primary nematode sensory organ, the amphid, consists of twelve bilaterally symmetric amphid neuron pairs that function to detect chemicals, touch and

temperature. Each amphid neuron has a single axon that extends in the nerve ring and a ciliated sensory dendrite that connects to an opening in the anterior cuticle (White et al., 1986). Most amphid axons reach the nerve ring after first growing ventrally in the amphid commissure, while one pair projects directly to the ring in a lateral position. The navigation of sensory axons in the nerve ring is largely completed by the end of embryogenesis. However, nerve ring axons continue to grow as the animal grows during the larval stages. During larval development, nerve ring axons increase 2.5-fold in length, while retaining the spatial organization established during embryogenesis. In the nerve ring, amphid sensory axons contact sensory and interneuron targets, establishing neural circuits essential to sensation and behavior (White et al., 1986).

While little is known about the genes that direct amphid axon guidance, three cytoplasmic proteins are required for amphid axon extension: UNC-33/CRMP, UNC-44/ankyrin and UNC-76 (Hedgecock et al., 1985; Siddiqui and Culotti, 1991; McIntire et al., 1992; Otsuka et al., 1995; Bloom and Horvitz, 1997). In addition, the INA-1 α -integrin is required for amphid axon fasciculation (Baum and Garriga, 1997). Axon growth and maintenance in the larval stages may have requirements that are distinct from initial axon development. For some amphid sensory neurons, maintenance of axon morphology is regulated by neuronal electrical activity (Coburn and Bargmann, 1996; Coburn et al., 1998; Peckol et al., 1999).

To obtain information about the mechanisms of axon extension, guidance and maintenance in the *C. elegans* nerve ring, we conducted screens for mutants with altered trajectories of nerve ring sensory axons. We isolated mutations in 12 genes, including 8 new genes. Some mutations disrupted the initial outgrowth and guidance of axons in the nerve ring, as well as in other locations, while other mutations disrupted later aspects of nerve ring maintenance. In addition, we found that the SAX-3/Robo, VAB-1/Eph receptor and UNC-6/netrin, UNC-40/DCC guidance systems function together to guide sensory axons ventrally in the amphid commissure.

MATERIALS AND METHODS

Strain maintenance

Animals were maintained using standard methods (Brenner, 1974). Unless noted, *sax-3(ky123)*, *ky198*, *ky203*, *sax-5*, *sax-7* and *sax-8* were grown at 20°C, and *sax-1*, *sax-2*, *sax-3(ky200ts)*, *sax-6*, *sax-9* and *sax(ky213)* were grown at 25°C, where their defects were more severe. All *sax-3* alleles showed decreased viability at 25°C.

Strain construction

Details of plasmid construction are available upon request. Briefly, the *ceh-23::gfp* transgene contains a promoter and coding region fragment of the *ceh-23* gene (Wang et al., 1993) fused to a peptide from *unc-76* (Bloom and Horvitz, 1997) followed by the *gfp* coding region (Chalfie et al., 1994). The *ceh-23::gfp* construct was introduced into a *lin-15(n765ts)* mutant strain with the *lin-15* plasmid pJM23 (Huang et al., 1994) by germline transformation, and stable transgenic strains were generated by gamma irradiation as described (Mello and Fire, 1995) to generate *kyIs4*. *kyIs4* was outcrossed six times and mapped to LGXR. In *kyIs4*, GFP expression was consistently observed in the following neuron pairs: ADF, ADL, AFD, ASE, ASG, ASH, AWC and occasionally ASI in the amphid, BAG and AIY in the head, CAN in the central body, and PHA and PHB in the tail. *kyIs4* animals exhibited wild-type amphid neuron morphology (White et al.,

1986) and normal chemotaxis responses to the odorants benzaldehyde, 2-butanone and isoamyl alcohol, indicating that the AWC neurons were functional (Bargmann et al., 1993).

The *mec-7::sax-3* transgene contains a partial *sax-3* cDNA (nucleotides 1-1343) followed by the *sax-3* genomic region containing the rest of the *sax-3* open reading frame and part of the *sax-3* 3' UTR cloned into the ppD96.41 *mec-7* promoter vector (A. Fire and S. Xu, personal communication). The *mec-7::sax-3* construct was injected at 10 ng/ μ l into *sax-3(ky123)* with 50 ng/ μ l of *str-1::gfp* as a coinjection marker.

Visualization of neuronal morphology

For DiI staining of amphid neurons, adult animals were exposed to a 15 μ g/ml solution of DiI in M9 buffer for 1.5 hours. DiO staining was conducted as previously described (Coburn and Bargmann, 1996). These techniques label the ADL, ASH, ASI, ASJ, ASK and AWC amphid neuron pairs. To visualize other neuron types, we used the *str-3::gfp* transgene *kyIs128* X (ASI sensory neurons in the head; E. Troemel and C. I. B., unpublished results) the *glr-1::gfp* transgene *kyIs29* X (interneurons and motor neurons in the nerve ring and ventral nerve cord; Maricq et al., 1995) and the *mec-4::gfp* transgene *bzIs7* IV (touch sensory neurons in the body; E. Wu and M. Driscoll, personal communication). The HSN neurons in the central body were visualized with antibodies to serotonin (Desai et al., 1988) in mutant strains that did not contain a *gfp* transgene.

Fluorescent animals were examined using a Zeiss Axioplan microscope and images assembled using Adobe Photoshop. Confocal images in Fig. 2 were generated from optical sections collected on a Zeiss LSM410 Invert confocal microscope and three-dimensional reconstructions were created using NIH Image 1.61/ppc.

Chemotaxis enrichment screen

kyIs4 animals were mutagenized with EMS (Brenner, 1974). Mutagenized animals were grown at 25°C for two generations and their F₂ progeny assayed for chemotaxis to a point source of 5 nl benzaldehyde (Bargmann et al., 1993). After 1 hour, animals at the benzaldehyde source were removed and the remaining animals scored by fluorescence. *sax-3*, *sax-5*, *sax-7*, *sax-8* and *unc-44(ky110)*, *ky115*, *ky116*, *ky186*, *ky256* alleles were obtained in the chemotaxis enrichment screen. Mutants were backcrossed three times by *kyIs4* and once by N2 to separate the *sax* mutation from the *ceh-23::gfp* transgene. DiO staining detected similar amphid phenotypes in mutants with or without *ceh-23::gfp*.

daf-11 suppression screen

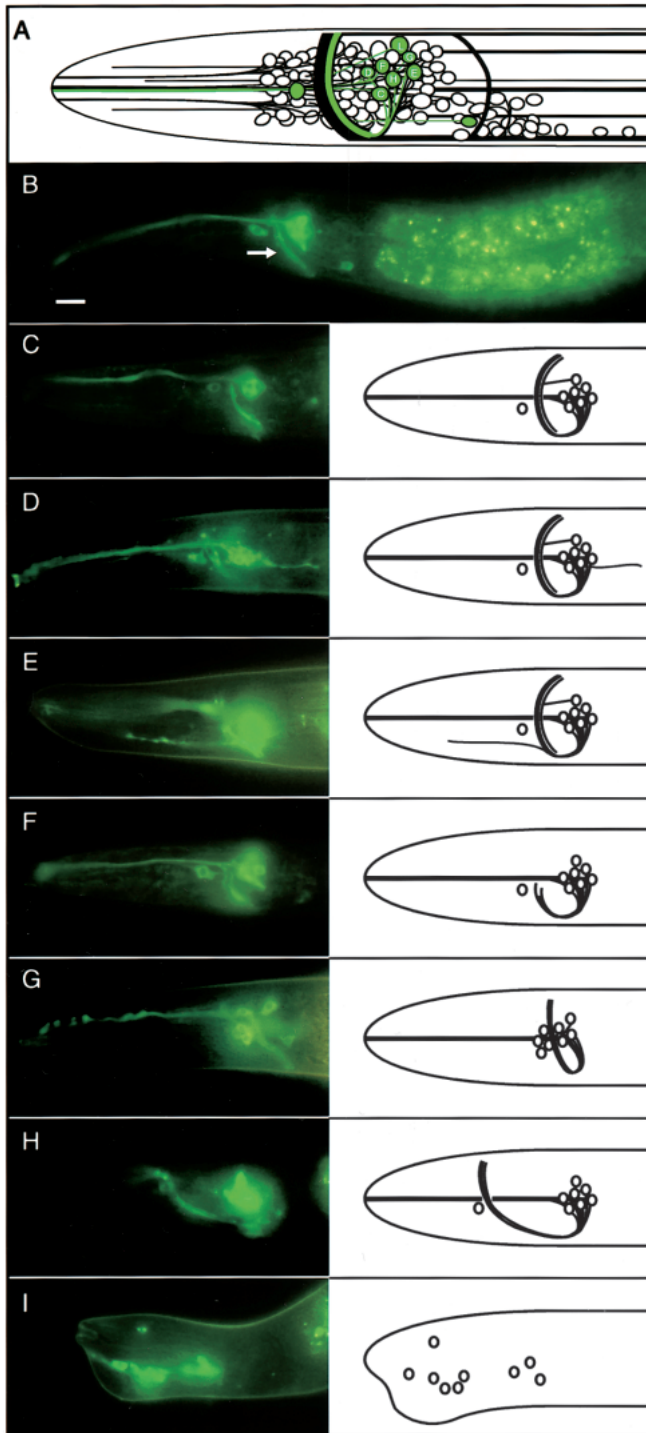
daf-11(m47) V; *kyIs4* X and *daf-11(m84)* V; *kyIs4* X strains were mutagenized with EMS and grown for one generation at 15°C. F₁ progeny were shifted to 25°C as L4 larvae and F₂ nondauers were cloned and their progeny scored for axon defects by fluorescence. *sax-1*, *sax-2*, *sax-9*, *unc-33*, *unc-44(ky257)* and *unc-76* alleles were isolated as suppressors of *daf-11(m47)*. *sax-6* and *sax(ky213)* were isolated as suppressors of *daf-11(m84)*. Mutations were not retested for suppression of *daf-11*. Mutants were outcrossed by a *him-5(e1490)* V; *kyIs4* X strain to replace *daf-11* with the closely linked *him-5* mutation. Mutant *him-5* strains were outcrossed twice by *kyIs4* to separate the *sax* mutation from *him-5* and once by N2 to separate the *sax* mutation from the *ceh-23::gfp* transgene. *unc-76(ky258)* was not separated from the *daf-11* mutation.

Mapping

All *sax* mutations were recessive. Their genomic locations were determined by mapping with respect to recessive and dominant genetic markers. Details of mapping are available upon request. Mutations were followed using the amphid axon phenotype detected by *ceh-23::gfp* or DiO staining.

sax-1 mapped to X under the *mnDp57* duplication. *sax-2* mapped to III to the left or close to *dpy-17* (0/4 *dpy-17* non *unc-32* recombinants

and 15/15 *unc-32* non *dpy-17* recombinants were mutant). *sax-3(ky123)* mapping is described in Zallen et al. (1998). *sax-5* mapped to IV between *unc-26* and *dpy-4* (13/19 *dpy-4* non *unc-26* recombinants were mutant). *sax-6* mapped to I (5/7 non *bli-3 unc-54* isolates were mutant and 2/7 were heterozygous). *sax-7* mapped to IV to the left or close to *unc-24* (0/7 *unc-24* non *dpy-20* recombinants and 1/1 *dpy-20* non *unc-24* recombinants were mutant). *sax-8(ky201)* mapped to III between *dpy-17* and *unc-32* (1/4 *dpy-17* non *unc-32* recombinants and 4/6 *unc-32* non *dpy-17* recombinants were mutant). *sax-9(ky218)* mapped to IV to the left or close to *unc-26* (0/11 *unc-26* non *dpy-4* recombinants were mutant). *kyls4* mapped to XR to the left of *unc-3* (1/12 *unc-3* non *lon-2* recombinants had *kyls4*).



RESULTS

Identification of mutants with sensory axon defects

To visualize nerve ring axons in living animals, we used the *ceh-23* cell-specific promoter (Wang et al., 1993) to express the green fluorescent protein (GFP). The *ceh-23::gfp* fusion was expressed in nine pairs of neurons in the head, including seven amphid neuron pairs (Fig. 1A,B), the BAG sensory neurons and the AIY interneurons, as well as the CAN neuron pair in the central body (Fig. 4A). The *ceh-23::gfp* transgene did not appear to disrupt the position, morphology or function of these neurons (Materials and Methods).

Behavioral and developmental assays that require amphid sensory function were used to enrich for mutations that disrupt amphid neuron development (Materials and Methods). In one screen, mutagenized animals were tested for chemotaxis to an odorant sensed by the AWC amphid neurons to identify chemotaxis-defective and movement-defective mutants. These animals were then screened visually for altered morphology of *ceh-23::gfp*-labeled neurons. A second screen made use of *daf-11* mutants, which are growth arrested in the dauer larval stage (Riddle et al., 1981). Dauer formation occurs in response to sensory stimuli, and disruption of amphid neuron function suppresses the constitutive dauer arrest of *daf-11* mutants (Vowels and Thomas, 1992; Schackwitz et al., 1996; Coburn

Fig. 1. Amphid axon trajectories in wild-type (A-C) and *sax* mutant animals (D-I), labeled by the *ceh-23::gfp* transgene. (A) Schematic diagram of the anterior nervous system of *C. elegans*. Anterior is to the left, dorsal at top. Neurons and processes are indicated. The main process bundle is the nerve ring (arrow in B), with ~100 axons in a typical cross section (White et al., 1986). Neurons that express the *ceh-23::gfp* transgene are shown in green. This lateral view shows one member of each bilaterally symmetric neuron pair. GFP expression is detected in the amphid sensory neurons ADF, ADL, AFD, ASE, ASG, ASH and AWC, each indicated by the last letter of its name. The BAG and AIY neurons in the head also express *ceh-23::gfp*. Most amphid axons first project ventrally through the amphid commissure to enter the nerve ring in a ventral position and then travel dorsally within the nerve ring to the dorsal midline. The ASE and AWC axons continue around the ring to terminate laterally on the other side. The ADL axon extends directly to the nerve ring in a lateral position and then branches, with the two branches extending within the nerve ring to the dorsal and ventral midlines, respectively. (B) The *ceh-23::gfp* transgene labels amphid sensory neurons, shown here in a larval (L4) stage animal. GFP expression is detected in the cell bodies (excluded from the nucleus), axons and dendrites of labeled cells. The axons travel circumferentially in the nerve ring neuropil. Similar GFP expression is observed in all larval stages and the adult. Autofluorescence from the gut is present in the body of the animal. Scale bar = 10 μ m. (C-I) Amphid neuron morphology in adult wild-type (C) or *sax* mutant animals (D-I). (C) Wild-type amphid axons extend in the nerve ring; about half of the nerve ring can be seen in this plane of focus. (D) An aberrant posteriorly misdirected process in a *sax-2* mutant. (E) An aberrant anteriorly misdirected axon in a *sax-3(ky123)* mutant. (F) Premature axon termination in the nerve ring in a *vab-3(ky112)* mutant. Most axons terminate in a ventral position, while two axons terminate in more lateral positions. (G) The nerve ring is displaced posteriorly relative to the amphid cell bodies in a *sax-7* mutant. Several additional cells are now anterior to the nerve ring. (H) Anteriorly displaced nerve ring in a *sax-3(ky123)* mutant. (I) Abnormal head morphology in a *sax-3(ky123)* mutant. Note that the cell bodies are in more anterior positions than in wild type.

Table 1. Genes required for normal amphid axon trajectories

Gene (alleles)	Linkage Group	Movement
Posteriorly misdirected axons		
<i>sax-1(ky211)</i> ¹	X	wild-type
<i>sax-2(ky216)</i> ¹	III	wild-type
<i>sax-6(ky214)</i> ¹	I	wild-type
<i>sax(ky213)</i> ²		wild-type
Anteriorly-misdirected axons		
<i>sax-3(ky123, ky198, ky200, ky203)</i>	X	mild kinker and coiler Unc
Premature axon termination		
<i>sax-5(ky118)</i>	IV	kinker Unc
<i>unc-33(ky255)</i>	IV	immobile Unc
<i>unc-44(ky110, ky115, ky116, ky186, ky256, ky257)</i>	IV	immobile Unc
<i>unc-76(ky258)</i>	V	immobile Unc
Altered nerve ring placement		
<i>sax-7(ky146)</i>	IV	wild-type
<i>sax-8(ky188, ky199, ky201)</i>	III	wild-type
Multiple defects		
<i>sax-9(ky212, ky218)</i> ¹	IV	mild kinker Unc
¹ <i>sax-1, sax-2, sax-3(ky200), sax-6</i> and <i>sax-9</i> mutants were temperature sensitive. Unless otherwise noted, these mutants were scored at 25°C.		
All other mutants were scored at 20°C.		
² The <i>sax(ky213)</i> mutant phenotype was too weak for linkage mapping.		

et al., 1998). Mutagenized *daf-11* animals were screened for suppressed mutants that relieved the *daf-11* arrest and reached adulthood. These mutants were then examined visually for defects in axon morphology.

We screened 27,000 genomes using the chemotaxis enrichment strategy and isolated 15 mutations in six genes, determined by map position and complementation testing. We screened 6,000 genomes in the *daf-11* suppression screen and isolated 9 mutations in at least seven genes. These screens

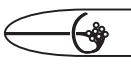



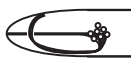
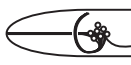
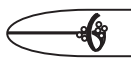
identified different sets of genes, except for one gene isolated in both screens (Table 1). The new genes were designated *sax* genes (for sensory axon defects). These genes defined three main categories: (1) one gene required for nerve ring axon guidance (*sax-3*), (2) three genes required for both nerve ring axon extension and guidance (*sax-5, sax-9* and *unc-44*), and (3) five genes where initial development proceeded normally, but defects occurred in the subsequent maintenance of nerve ring morphology (*sax-1, sax-2, sax-6, sax-7* and *sax-8*).

sax-3/robo mutations disrupt multiple aspects of amphid axon guidance

Mutations in the *sax-3/robo* gene, a transmembrane protein that may function as a guidance receptor, caused amphid axons to extend inappropriately into the region anterior of the nerve ring (Fig. 1E,H; Table 2). As few as one or as many as all *ceh-23::gfp*-labeled axons extended anteriorly in an individual mutant animal. When all seven labeled axon pairs were anteriorly misrouted, they were often able to complete the dorsal component of their trajectories, forming an anteriorly displaced structure that resembled the nerve ring. All amphid neurons labeled by the *ceh-23::gfp* transgene or the fluorescent dyes DiO and DiI exhibited defects in *sax-3* mutants, indicating that mutations in *sax-3* disrupted the pathfinding of at least 11 of the 12 amphid neuron pairs. In addition, nerve ring axons from eight classes of interneurons and three classes of motor neurons labeled by the *glr-1::gfp* transgene (Maricq et al., 1995) also exhibited anterior axons (97% defective in *sax-3(k123)*, *n*=31), indicating that *sax-3* is likely to affect the position of many or all nerve ring axons.

The severity of the amphid axon defects prompted us to examine the trajectories of individual axons in *sax-3* mutants. The *str-3::gfp* transgene specifically labels the two ASI amphid

Table 2. Amphid axon defects in sax mutants

Genotype								n
Wild type	100%							300
posterior processes								
<i>sax-1(ky211)</i> 20°C	76%					24%		130
<i>sax-1(ky211)</i> 25°C	36%					64%		190
<i>sax-2(ky216)</i> 20°C	89%					11%		103
<i>sax-2(ky216)</i> 25°C	54%					46%		134
<i>sax-6(ky214)</i>	80%					20%		376
<i>sax(ky213)</i>	92%					8%		95
anterior processes								
<i>sax-3(ky123)</i> ^{2, 3}	16%		25%	13%	60%	9%		55
axon termination								
<i>sax-5(ky118)</i>	7%	81%		2%		48%		42
<i>unc-44(ky116)</i>		90%		7%		90%		30
altered nerve ring placement								
<i>sax-7(ky146)</i>	4%			2%			94%	50
<i>sax-8(ky201)</i> ²	41%						59%	29
multiple defects								
<i>sax-9(ky212)</i> ²	67%	11%	16%	4%		13%		45

Amphid axon phenotypes were characterized in adults with the *ceh-23::gfp* marker. Schematic drawings show the head of the animal. Anterior is to the left, dorsal at top. *n* = number of animals scored. Mutants characterized at multiple temperatures are indicated. Animals with more than one phenotype were scored in multiple categories, so percentages do not always add up to 100%.

¹In these mutants, all amphid axons were found in an abnormal location with respect to their cell bodies.

²All alleles of *sax-3, sax-8* and *sax-9* had similar amphid defects.

³Axons were scored only when the amphid cell bodies were correctly positioned.

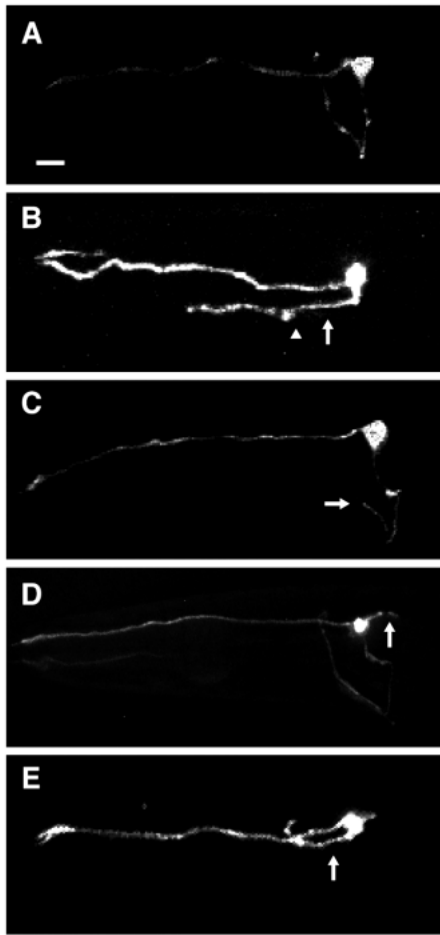


Fig. 2. ASI axon trajectories in wild-type (A) and *sax* mutant animals (B–E), labeled by the *str-3::gfp* transgene. Anterior is to the left, dorsal at top. Scale bar, 10 μ m. (A) The wild-type ASI axon first projects ventrally to the ventral midline and then dorsally in the nerve ring. The ASI axon continues around the ring to terminate near the dorsal midline; only one side of the animal is shown in these confocal images. (B) In a *sax-3(ky200)* mutant, the ASI axon fails to grow ventrally in the amphid commissure and extends directly to the nerve ring in a lateral position (arrow). In addition, the axons continue past the position of the nerve ring (arrowhead) and into the anterior head region. (C) In a *sax-5(ky118)* mutant, the ASI axon terminates prematurely (arrow). (D) In a *sax-2(ky216)* mutant, the primary axon extends normally in the nerve ring. In addition, an ectopic neurite (arrow) travels in a posterior direction. (E) In an *unc-40(ev271)* mutant, the ASI axon grows directly to the nerve ring in a lateral position (arrow).

neurons (E. Troemel and C. I. B., unpublished data), each of which projects a single axon ventrally to the ventral midline in the amphid commissure and then dorsally within the nerve ring (Fig. 2A). In *sax-3* mutants, the ASI axons often deviated anteriorly from their normal trajectory in the nerve ring (Fig. 2B; Table 3) or failed to grow ventrally in the amphid commissure and instead projected directly to the nerve ring in a lateral position. These laterally misrouted axons either continued dorsally in the nerve ring or terminated in a lateral position, perhaps because of a failure to encounter their normal substrata for nerve ring entry. A similar defect in the ventral guidance of six amphid neuron pairs was detected by DiI

labeling (Fig. 5). These results indicate that *sax-3* is required for two distinct guidance decisions of amphid sensory axons: first to guide amphid commissure axons ventrally to the nerve ring entry point and then to prevent axons in the nerve ring from wandering anteriorly.

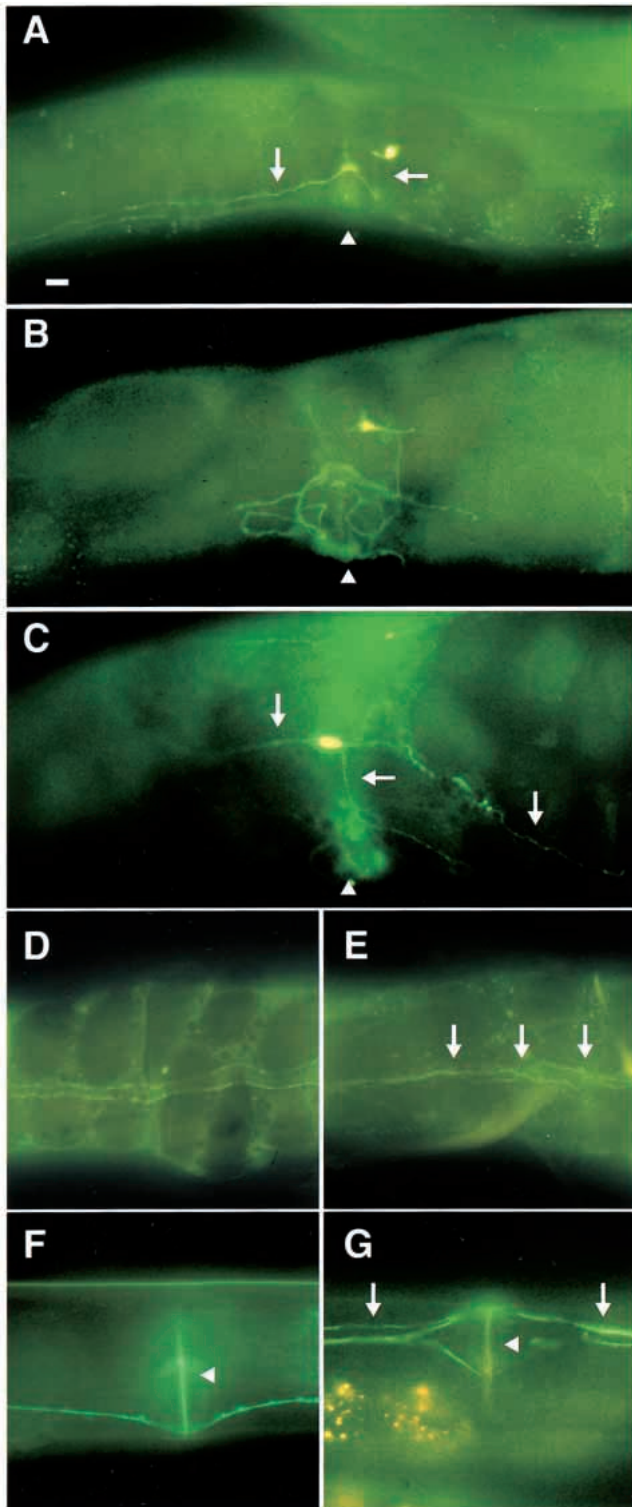
sax-3 mutations also disrupted the cell migrations of some neuron types. Amphid neurons are born at the anterior tip of the animal and undergo short-range posterior migrations (Sulston et al., 1983). Amphid neurons were occasionally displaced anteriorly in *sax-3* mutants, consistent with a failure to complete their normal migrations (Fig. 1I, 22% of amphid neurons defective in *sax-3(ky123)* $n=55$). In addition, *sax-3* mutants exhibited defects in two long-range cell migrations, the posterior migration of the CAN neurons (Fig. 4B; Table 5) and the anterior migration of the HSN motor neurons (7% defective in *sax-3(ky123)*, $n=27$). These phenotypes indicate that *sax-3* is required for cell migrations in both directions along the longitudinal axis.

sax-3 mutants also exhibited a number of other phenotypes. Defects in head morphology produced a notched head phenotype (Fig. 1I, 38% defective in *sax-3(ky123)* $n=71$). *sax-3* mutants exhibited a high incidence of embryonic lethality, with 82% of laid eggs ($n=150$) failing to hatch in the strong *sax-3(ky123)* allele (Zallen et al., 1998). The notched head phenotype and lethality are characteristic of mutants with defects in epithelial cell migration and adhesion (George et al., 1998). Consistent with the observation that *sax-3* mutations cause widespread neuronal defects, mutant animals were defective in a number of behaviors, including chemotaxis, locomotion and egg-laying.

***sax-5*, *sax-9* and *unc-44* mutations disrupt both extension and guidance of amphid axons**

Eleven mutations representing six genes caused amphid sensory axons to terminate prematurely before completing their trajectories in the nerve ring (Figs 1F, 2C; Tables 2, 3). In these mutants, most axons arrived at the nerve ring as in wild type, but terminated within the ring before reaching the dorsal midline. These mutants include three previously identified genes, *unc-33*, *unc-44* and *unc-76*, which are required for axon outgrowth in several neuron classes, including amphid neurons (Hedgecock et al., 1985; Desai et al., 1988; Siddiqui, 1990; Siddiqui and Culotti, 1991; McIntire et al., 1992). In addition, a gene originally designated *sax-4(ky112)* was found to be allelic to the *vab-3* gene (J. Hao, E. Lundquist, J. A. Z. and C. I. B., unpublished data). *vab-3* encodes a Pax family transcription factor (Chisholm and Horvitz, 1995) and characterization of *vab-3* alleles revealed severe defects in amphid axon extension (Fig. 1F, 63% defective in *vab-3(e648)*, $n=99$ by DiI labeling).

Mutations in *sax-5*, *sax-9* and *unc-44* caused defects in amphid axon guidance as well as extension (Table 2). In *sax-5* and *unc-44* mutants, nearly all axons labeled by *ceh-23::gfp*, DiO and *str-3::gfp* were defective, suggesting that these mutations affect at least 11 of the 12 amphid neuron pairs. Both *sax-5* and *unc-44* mutants retained a ring of motor neuron and interneuron axons that express *glr-1::gfp* around the circumference of the nerve ring, excluding the possibility that these mutations cause a complete loss of the nerve ring. Mutations in *sax-9* caused lower penetrance defects in amphid axon extension and guidance (Table 2).



Mutations in *sax-5*, *sax-9* and *unc-44* also caused misrouting of the HSN motor axon (Table 4), consistent with a role for these genes in axon pathfinding. In wild-type animals, the two HSN neurons in the central body region each project a single axon ventrally to the ventral midline and then anteriorly to the head (Fig. 3A). In *sax-5*, *sax-9* and *unc-44* mutants, the HSN axon often grew in a lateral position or wandered and branched extensively in the vicinity of the cell body (Fig. 3B). In some animals, the HSN axon grew posteriorly instead of anteriorly

Fig. 3. HSN and interneuron axon trajectories in wild-type (A,D,F) and *sax* mutant animals (B,C,E,G), labeled with antibodies to serotonin (A-E) or the *glr-1::gfp* transgene (F,G). Anterior is to the left, lateral view (A-C) or ventral view (D-G). Scale bar, 10 μ m. Arrowhead in all parts denotes the vulva. (A) HSN morphology in a wild-type animal. The HSN cell body is located in the midbody. The HSN axon (arrows) extends ventrally to the vulva, where it forms a branch and extends anteriorly in the ventral nerve cord. (B) In a *sax-5(ky118)* mutant, the HSN axon first grows ventrally, then wanders and branches extensively in the vicinity of the vulva without reaching the ventral cord. (C) In an *unc-44(ky110)* mutant, three axons (arrows) project from the HSN cell body. One axon extends ventrally as in wild type, but terminates prematurely at the vulva. Additional axons grow in aberrant lateral positions in anterior and posterior directions. The anteriorly directed axon wanders dorsally and posteriorly before terminating. (D) In a wild-type ventral view, the two HSN axons travel on opposite sides of the ventral midline, shown here immediately anterior to the vulva (out of view at right). (E) In a *sax-5(ky118)* mutant, the HSN axons cross and recross the midline, often traveling together on one side of the ventral cord (arrows). (F) In a wild-type ventral view, eleven interneuron axons travel on the right side of the ventral midline. (G) In a *vab-1(dx31)* mutant, these axons aberrantly cross over to the left side of the ventral cord (arrows).

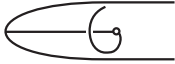



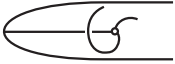
in the ventral cord, and when the axon did grow anteriorly as in wild type, it often terminated prematurely. Consistent with previous reports, *unc-44* mutants also exhibited defects in HSN axon outgrowth, leading to premature termination (Table 4; McIntire et al., 1992). Axon termination was also observed in the CAN neurons in the central body (Table 5). In addition, *unc-44* mutants exhibited ectopic HSN axons, with up to four axons from a single neuron, suggesting a role for *unc-44* in axon initiation (Fig. 3C; Table 4). Ectopic axons were also observed in *unc-33(e204)* mutants (data not shown).

sax-5 and *sax-9* mutations also disrupt axon guidance in the ventral nerve cord, the second largest axon bundle in *C. elegans*. The ventral nerve cord is normally asymmetric; over 30 axons travel on the right side of the ventral midline, while only 4-6 axons travel on the left side (White et al., 1976). The decision to join one side of the ventral cord is made upon arrival at the ventral midline, and axons in the body region do not cross the midline subsequent to this choice. When the HSN axon arrives at the ventral midline, it joins the ipsilateral cord and travels anteriorly to the head. While wild-type HSN axons travel on opposite sides of the ventral cord (Fig. 3D), axons often traveled together on the same side in *sax-5* and *sax-9* mutants (Fig. 3E; Table 4). Similarly, eleven *glr-1*-expressing interneuron axons that normally extend in the right ventral cord occasionally grow on the left side in *sax-5* mutants (Table 4). Mutations in both *sax-5* and *sax-9* also disrupted the posteriorly directed CAN cell migrations (Fig. 4C; Table 5), while only mutations in *sax-9* disrupted the anteriorly directed HSN migration (7% defective, $n=110$). Cell migration defects were not observed in *unc-33*, *unc-44* or *unc-76* mutants.

***sax-1*, *sax-2* and *sax-6* mutations disrupt the maintenance of neuronal morphology**

Mutations in the *sax-1*, *sax-2* and *sax-6* genes caused amphid neurons to send aberrant processes into the region posterior to the nerve ring (Fig. 1D). The *ceh-23::gfp* marker detected one to several aberrant posteriorly directed processes per amphid,

Table 3. Axon defects in the ASI amphid neurons

						n
	Wild type	Axon termination	Lateral axon	Anterior axon	Ectopic neurite	
WT	100%					300
<i>sax-1(ky211)</i>	55%				45%	267
<i>sax-2(ky216)</i>	26%				74%	364
<i>sax-3(ky200)</i> 20°C	97%	3%				104
<i>sax-3(ky200)</i> 25°C	20%	14%	23%	59%		132
<i>sax-5(ky118)</i>	1%	99%				300
<i>unc-6(ev400)</i>	71%	12%	17%			386
<i>unc-40(e1430)</i>	84%	10%	6%			300
<i>unc-40(e271)</i>	91%	4%	5%			300
<i>unc-40(n324)</i>	90%	3%	7%			314
<i>unc-5(e53)</i>	99%		1%			622
<i>vab-1(dx31)</i>	41%		59%			41

Amphid axon phenotypes were characterized in adults using the *str-3::gfp* marker. Schematic drawings show the head of the animal. Anterior is to the left, dorsal at top. n = number of neurons scored. Mutants scored at multiple temperatures are indicated. Animals with more than one phenotype were scored in multiple categories, so percentages do not always add up to 100%.

Fig. 4. CAN neuron positions in wild-type (A) and *sax* mutant animals (B,C), labeled with the *ceh-23::gfp* transgene. Anterior is to the left, dorsal at top. The nerve ring in the head of the animal is marked with an arrowhead. (A) CAN morphology in a wild-type animal. The CAN cell body migrates posteriorly from the head to its final position in the midbody of the animal (arrow). One CAN axon travels anteriorly to the head in a lateral position, while the other travels posteriorly to the tail (not shown). (B) The CAN cell body is observed in a more anterior position in a *sax-3(ky123)* mutant (arrow). The posterior CAN axon is unaffected, although it leaves the plane of focus in this photograph. The anterior CAN axon travels to the head as in wild type. (C) The CAN cell body is observed in the head of a *sax-5(ky118)* mutant. The posterior CAN axon is unaffected. It was not possible to score the anterior CAN axon.

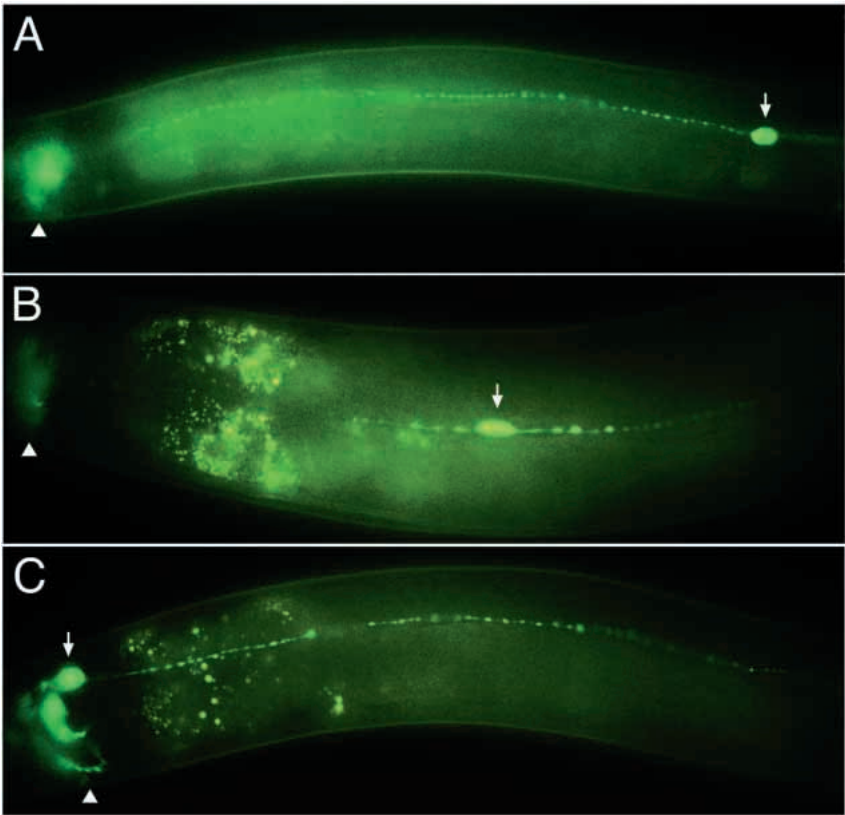


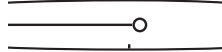

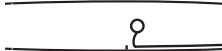

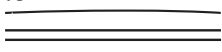
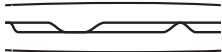




Table 4. Ventral guidance and midline crossover defects in *sax* mutants

	WT	<i>sax-5</i>	<i>sax-9</i> ³	<i>vab-1</i> ³	<i>unc-44</i> ³
Wild-type HSN (lateral view)		100%	6%	85%	99%
Defects in ventrally-directed growth axon wandering/branching		26%	9%		30%
lateral axon ¹		3%	5%	1%	59%
Defects in anteriorly-directed growth termination of anterior axon		37%			54%
posterior axon ²		57%	5%		84%
Ectopic axons		3%			57%
	n = 70	n = 35	n = 97	n = 185	n = 37
Wild-type HSN (ventral view)		98%	38%	68%	49%
Axon crossover		2%	62%	32%	51%
	n = 63	n = 34	n = 31	n = 126	ND
Wild-type <i>glr-1::GFP</i> (ventral view)		100%	96%	92%	97%
Axon crossover			4%	8% ⁴	3%
	n = 121	n = 85	ND	n = 100	n = 75

Axon phenotypes were scored in adults stained with anti-serotonin antibodies (HSN motor neurons) or the *glr-1::gfp* marker (ventral cord interneurons). Schematic drawings show the central third (top and bottom panels) or anterior third (middle panel) of the animal. Anterior is to the left. Animals with more than one phenotype were scored in multiple categories, so numbers do not always add up to 100%. n = number of neurons (top panel), axon segments (middle panel) or animals (bottom panel) scored.

¹ The lateral axon category included axons that grew in anterior or posterior directions.

² The posterior axon category included axons that grew in ventral or lateral positions.

³ Alleles scored were *sax-9(ky212)*, *vab-1(e2)* (HSN), *vab-1(dx31)* (*glr-1::gfp*), *unc-44(ky116)* (HSN) and *unc-44(ky145)* (*glr-1::gfp*). Similar HSN defects were observed in *vab-1(dx31)*, *unc-44(e362)* and *unc-44(ky110)*.

⁴ The *vab-1(dx31)* *glr-1::gfp* crossover defect differs significantly from wild type (p=0.005, Chi-square test).

in addition to a set of apparently normal axons in the nerve ring. Defects were observed both with the *ceh-23::gfp* transgene and with DiO and DiI filling, where some aberrant processes were traceable to the ASJ neuron. *sax-1*, *sax-2* and *sax-6* were identified as suppressors of *daf-11* dauer constitutivity, an assay that can detect subtle sensory defects. Laser ablation of the ASJ neuron pair suppresses the dauer arrest of *daf-11* mutant animals (Schackwitz et al., 1996).

Therefore, it is possible that the ASJ axon defects in these mutants altered ASJ function. To characterize the behavior of individual axons in *sax-1* and *sax-2* mutants, we examined the ASI neuron pair. In all cases, the posteriorly directed processes were found to be ectopic neurites, since each ASI neuron also extended an apparently normal axon in the nerve ring (Fig. 2D; Table 3). To determine whether the phenotypes in *sax-1* and *sax-2*

Table 5. CAN cell migration and axon outgrowth defects in *sax* mutants

	WT	<i>sax-3</i> ²	<i>sax-5</i>	<i>sax-9</i> ²	<i>unc-44</i> ²
wild-type CAN	100% ¹	10%	51%	52%	100%
>1/2 normal migration distance ³		37%		3%	
≤1/2 normal migration distance ³		53%	49%	45%	
axon termination		post. 4%	post. 6%		ant. 100% post. 100%
	n = 100	n = 30	n = 67	n = 31	n = 31

CAN axon outgrowth and cell migration phenotypes were characterized in adults with the *ceh-23::gfp* transgene. Schematic drawings show the entire animal. Anterior is to the left, dorsal at top. n = number of neurons scored. No CAN cell migration or axon outgrowth defects were observed in *sax-1*, *sax-2*, *sax-6*, *sax-7* or *sax-8* mutants.

¹ The wild-type strain used for comparison was the *ceh-23::gfp* strain *kyIs4*. *kyIs4* control animals exhibited low penetrance CAN cell displacement, with 3/100 neurons migrating approximately 3/4 of the normal distance. Therefore, CAN neurons were only scored as defective if the cell migrated less than 2/3 of the normal distance.

² Alleles scored were *sax-3(ky123)*, *sax-9(ky212)* and *unc-44(ky116)*. *sax-9(ky218)* and *unc-44(ky110)* caused similar defects.

³ In animals with CAN cell migration defects, the posterior CAN axon was almost always longer than or equal to its wild-type length: *sax-3* (96%, n=30), *sax-5* (94%, n=67) and *sax-9* (100%, n=31).

mutants reflect defects in the establishment or maintenance of neuronal morphology, we characterized the morphology of mutant neurons throughout development. While the outgrowth of amphid axons is completed by the end of embryogenesis, few ectopic neurites were detected by the *ceh-23::gfp* transgene in first-stage (L1) larval *sax-1* and *sax-2* mutant animals, and aberrant neurites increased in penetrance during the later larval stages (data not shown). These results are consistent with a role for *sax-1* and *sax-2* in the maintenance of neuronal morphology during larval growth.

The *sax-1* and *sax-2* mutant phenotypes were not specific to amphid sensory neurons, since aberrant ectopic neurites were also observed in the CAN neurons (29% in *sax-1*, n=121; 53% in *sax-2*, n=36) and *glr-1::gfp*-labeled inter- and motor neurons (46% in *sax-1*, n=54; 39% in *sax-2*, n=31). However, the cell migrations and guidance of the primary axons of amphid, CAN, HSN and *glr-1::gfp*-labeled neurons were normal. Consistent with the observation that these aspects of neuronal morphology are preserved in these mutants, mutant animals performed normally in a range of behavioral assays, including locomotion, egg-laying and osmotic avoidance (data not shown).

***sax-7* and *sax-8* mutations disrupt the maintenance of nerve ring placement**

In *sax-7* and *sax-8* mutants, the nerve ring contained an apparently normal complement of axons, and initial nerve ring morphology was wild type in postembryonic first-stage (L1) larvae. However, as mutant animals progressed through the four larval stages to adulthood, nerve ring axons became displaced posteriorly relative to the correctly positioned cell bodies (Fig. 1G; Table 2). *glr-1::gfp*-expressing axons of *sax-7* mutants were also posteriorly displaced (data not shown), indicating a general displacement of many or all nerve ring axons. However, no defects were observed in the ventral guidance of amphid axons in the amphid commissure (Fig. 1G;

Table 2), HSN motor axons or CAN axons. These phenotypes suggest a specific role for the *sax-7* and *sax-8* genes in the maintenance of nerve ring placement.

Mutations in multiple guidance pathways disrupt ventral guidance in the amphid commissure

To supplement genetic screens for new genes involved in *C. elegans* nerve ring development, we investigated whether mutations in known genes disrupted the trajectories of amphid sensory axons. The UNC-6/netrin secreted axon guidance cue and its receptor, UNC-40/DCC, are required for the guidance of many *C. elegans* axons along the dorsoventral axis (Hedgecock et al., 1990; Ishii et al., 1992; Chan et al., 1996). We found that, in *unc-6* and *unc-40* mutants, the ASI amphid axon sometimes failed to grow ventrally in the amphid commissure and instead traveled directly to the nerve ring in a lateral position (Fig. 2E; Table 3). In addition, other amphid axons labeled by DiI filling also exhibited ventral guidance defects (Fig. 5), indicating that, like *sax-3/robo*, *unc-6* and *unc-40* mutations disrupt the ventral guidance of multiple amphid neuron types. In mutant animals where ventral guidance occurred normally, amphid axons sometimes terminated prematurely while traveling dorsally in the nerve ring (Table 3; 17% defective in *unc-6(ev400)* n=240, 11% defective in *unc-40(e271)* n=332 by DiI filling). UNC-5, a transmembrane receptor that mediates repulsion from UNC-6 in combination with UNC-40 (Hedgecock et al., 1990; Leung-Hagesteijn et al., 1992; Hamelin et al., 1993), is not required for amphid axon guidance (Table 3; 1% defective in ventral guidance in *unc-5(e53)* by DiI filling, n=168).

Ventral guidance in the amphid commissure was also disrupted in animals mutant for VAB-1, a *C. elegans* Eph receptor that is expressed in neurons that project axons to the nerve ring (George et al., 1998). DiI filling revealed a partially penetrant defect in which many amphid axons grew directly to the nerve ring in a lateral position, a defect qualitatively

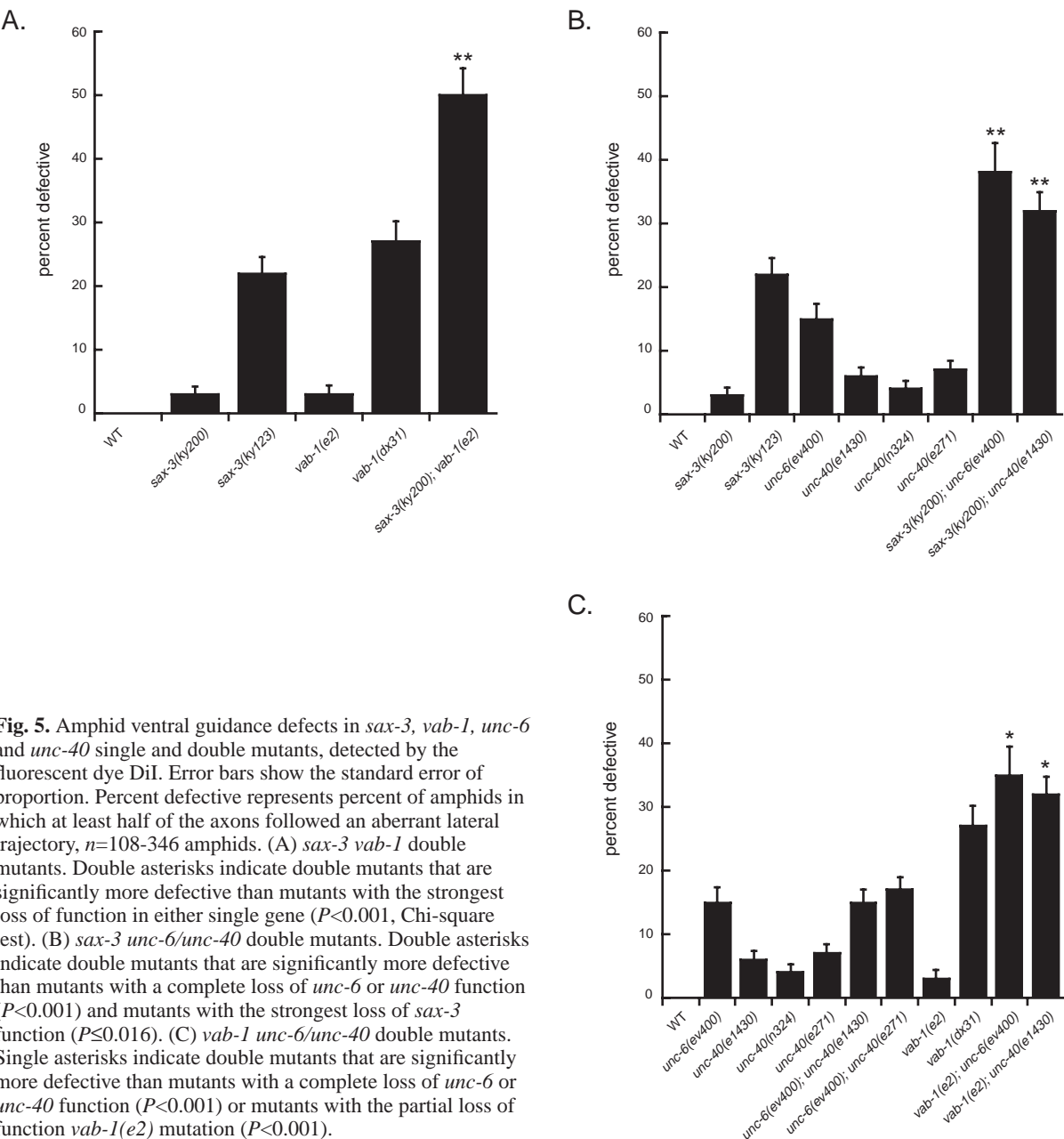


Fig. 5. Amphid ventral guidance defects in *sax-3*, *vab-1*, *unc-6* and *unc-40* single and double mutants, detected by the fluorescent dye DiI. Error bars show the standard error of proportion. Percent defective represents percent of amphids in which at least half of the axons followed an aberrant lateral trajectory, $n=108\text{--}346$ amphids. (A) *sax-3 vab-1* double mutants. Double asterisks indicate double mutants that are significantly more defective than mutants with the strongest loss of function in either single gene ($P<0.001$, Chi-square test). (B) *sax-3 unc-6/unc-40* double mutants. Double asterisks indicate double mutants that are significantly more defective than mutants with a complete loss of *unc-6* or *unc-40* function ($P<0.001$) and mutants with the strongest loss of *sax-3* function ($P\leq 0.016$). (C) *vab-1 unc-6/unc-40* double mutants. Single asterisks indicate double mutants that are significantly more defective than mutants with a complete loss of *unc-6* or *unc-40* function ($P<0.001$) or mutants with the partial loss of function *vab-1(e2)* mutation ($P<0.001$).

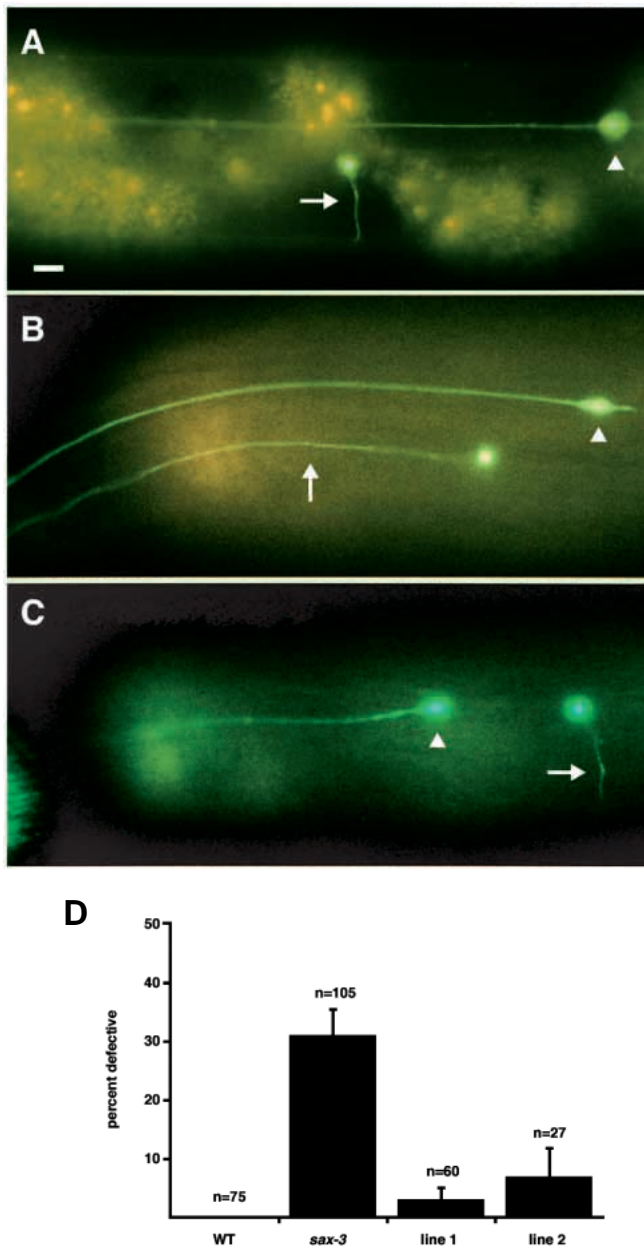
similar to the defects of *unc-6* and *unc-40* mutants (Fig. 5). *vab-1* mutants had a strong lateral axon phenotype in the ASI neuron, but no other ASI defects (Table 3). Amphid phenotypes were most severe in animals with the *vab-1(dx31)* deletion that removes the first four exons, but were also present in animals with the *vab-1(e2)* missense mutation that abolishes kinase activity (George et al., 1998). *vab-1* mutations caused minimal defects in ventral guidance of the HSN axons (Table 4).

Like SAX-3/Robo, the VAB-1/Eph receptor also affects axon guidance at the *C. elegans* ventral midline. In half of *vab-1(e2)* and *vab-1(dx31)* mutant animals, the HSN axon aberrantly crossed and recrossed the ventral midline (Table 4). Likewise, *glr-1*-expressing interneuron axons sometimes failed to remain in the right ventral cord and crossed over to the left side (Fig. 3G; Table 4).

SAX-3/Robo functions in parallel to VAB-1 and UNC-6/UNC-40 in the ventral guidance of amphid axons

SAX-3, UNC-6, UNC-40 and VAB-1 are all required for normal amphid axon trajectories; how do these molecules function together to guide axons ventrally in the amphid commissure? If these genes act in a single pathway, disrupting two genes should not cause a more severe defect than a complete loss of function in either one. Alternatively, if these genes act in parallel, then disrupting two genes together may cause a defect that is more severe than the defect in either single mutant.

The *vab-1(e2); sax-3(ky200)* double mutant was significantly more defective than animals lacking either *vab-1* or *sax-3* function (Fig. 5A). Similarly, double mutant combinations between *sax-3* and either *unc-6* or *unc-40* were significantly more defective than animals with strong



mutations in either *sax-3*, *unc-6* or *unc-40* (Fig. 5B). By contrast, *unc-40; unc-6* double mutants were not enhanced compared to *unc-6* single mutants (Fig. 5C), consistent with evidence that UNC-6 and UNC-40 participate in a single guidance pathway (Hedgecock et al., 1990). These results establish that the guidance functions of SAX-3/Robo do not absolutely require the VAB-1 Eph receptor or the UNC-6/netrin, UNC-40/DCC pathway.

The ventral guidance of amphid axons was significantly more defective in *vab-1(e2); unc-6(ev400)* or *unc-40(e1430); vab-1(e2)* double mutants than in *unc-6* or *unc-40* single mutants (Fig. 5C), indicating that the VAB-1 Eph receptor does not require UNC-6 or UNC-40 to execute guidance functions. However, the defects in double mutants with the weak *vab-1* allele did not exceed those caused by the strong *vab-1(dx31)* allele alone, so UNC-6 could participate in either a subset of VAB-1 activities or in a separate pathway. Unfortunately, the

Fig. 6. The *sax-3* AVM ventral guidance defect is rescued cell autonomously. AVM morphology was scored in adult and L4 animals using a *mec-4::gfp* transgene. Anterior is to the left, dorsal at top. Scale bar, 10 μ m. (A) AVM morphology in a wild-type animal. The AVM axon (arrow) grows ventrally to the ventral midline and then turns anteriorly in the ventral cord (out of the plane of focus). The ALMR neuron (arrowhead in all panels) also expresses *mec-4::gfp*. (B) In a *sax-3(ky123)* mutant, the AVM axon (arrow) fails to grow ventrally and instead extends anteriorly in a lateral position. (C) In a *sax-3(ky123)* mutant with a *mec-7::sax-3* transgene driving *sax-3* expression specifically in six cells including AVM, the AVM axon (arrow) grows ventrally as in wild type. (D) AVM ventral guidance defects in *sax-3(ky123)* mutants and two independent *sax-3(ky123); mec-7::sax-3* transgenic lines. Percent defective represents the percent of AVM neurons. Error bars show the standard error of proportion. Lines 1 and 2 were significantly different from *sax-3(ky123)* (line 1, $P < 0.001$; line 2, $P = 0.02$; Chi-square test). The AVM rescue was specific, as the *sax-3* amphid axon guidance defects were not rescued by the *mec-7::sax-3* transgene (*sax-3(ky123)*, 66% defective, $n = 105$ amphids; line 1, 65% defective, $n = 65$; line 2, 62% defective, $n = 63$).

lethality of double mutants precluded characterization of genetic combinations with strong loss-of-function *sax-3(ky123)* or *vab-1(dx31)* mutations.

***sax-3/robo* functions cell autonomously in ventral guidance of the AVM sensory axon**

The requirement for SAX-3/Robo in ventral guidance is consistent with two models: SAX-3 could act cell autonomously as a receptor on growing axons or non-autonomously, either as a receptor in another pioneer axon or as a ligand on the substratum. Since amphid axons grow out in the amphid commissure bundle, their ventral guidance may be achieved through the combined action of axon-axon and axon-substratum interactions. Like amphid neurons, the AVM mechanosensory neuron has a cell body that is located on the lateral hypodermis and an axon that grows ventrally to the ventral midline; however, the AVM axon travels independently using only axon-substratum interactions. For this reason, we chose to examine the question of *sax-3* autonomy in the AVM neuron. AVM, like amphid neurons, relies on *sax-3* for its ventral axon guidance (Fig. 6B,D) as well as *unc-6* and *unc-40* (Siddiqui, 1990; Chan et al., 1996).

To determine the site of *sax-3* action for AVM ventral guidance, we expressed the *sax-3* cDNA from the *mec-7* promoter, which drives expression in six mechanosensory neurons, including AVM (Hamelin et al., 1993). The *mec-7::sax-3* fusion rescued the AVM defects of *sax-3* mutants in two independent transgenic lines (Fig. 6C,D), indicating that SAX-3 can function cell autonomously in AVM ventral guidance. This result does not rule out the possibility that SAX-3 could behave non-autonomously in other cell contexts, such as the nerve ring.

DISCUSSION

Identification of genes required for normal sensory axon trajectories

Mutations in eight *sax* genes disrupt the trajectories of sensory axons in the *C. elegans* nerve ring. *sax-3/robo* is required for

two distinct guidance decisions in the amphid commissure and the nerve ring, while *sax-5*, *sax-9* and *unc-44* are required for nerve ring axon extension and guidance. Once amphid axons have completed their initial trajectories in the nerve ring, *sax-1*, *sax-2*, *sax-6*, *sax-7* and *sax-8* are required for the maintenance of nerve ring structure. Mutations in the *sax-3*, *sax-5*, *sax-9* and *unc-44* genes disrupt axon guidance or cell migration in other neuron types, indicating that their function is not limited to the nerve ring. Most of the *sax* mutants were not defective for locomotion, and therefore would not have been isolated in previous screens for axon guidance mutants in a collection of behaviorally uncoordinated mutants.

***sax-3*, *vab-1* and *unc-6/unc-40* function in parallel for ventral axon guidance**

The SAX-3/Robo, VAB-1/Eph receptor and UNC-6/netrin, UNC-40/DCC guidance systems are required to guide amphid sensory axons ventrally in the amphid commissure, but mutations in these genes cause relatively mild ventral guidance defects individually. Double mutants are more severe, suggesting that the SAX-3/Robo, VAB-1/Eph receptor and UNC-6/netrin, UNC-40/DCC pathways can function independently in ventral guidance, although these molecules may also share some functions. While the sequence and expression of SAX-3, UNC-40 and VAB-1 suggest that they could act as guidance receptors in nerve ring axons, cell autonomy studies will be required to determine the roles of these guidance molecules in the complex environment of the nerve ring.

The SAX-3/Robo immunoglobulin superfamily member functions cell autonomously in the AVM sensory neuron, consistent with a role as a receptor for ventral guidance. *sax-3* is expressed in amphid neurons as well as epidermal substratum cells during the time of amphid axon outgrowth in the embryo (Zallen et al., 1998). SAX-3 may act as a receptor for ventral guidance of amphid sensory neurons; alternatively, SAX-3 could function non-autonomously as a receptor in a nerve ring pioneer axon, as a ligand in an axon-substratum interaction, or in an earlier developmental process (see below). The UNC-40 guidance receptor is widely expressed in neurons (Chan et al., 1996). In the region of the nerve ring, its ligand UNC-6 is present in four neurons and two ventral CEP sheath cells that surround the amphid commissure, but is absent from the two dorsal CEP sheath cells (Wadsworth et al., 1996). This expression pattern suggests a model in which UNC-6 secreted by the ventral CEP sheath cells may attract axons from the amphid commissure that express the UNC-40 receptor. In this model, UNC-6 could act either as a diffusible chemoattractant or as a local substratum to direct axon growth.

The VAB-1 Eph receptor is expressed in many head neurons but not in their epidermal substratum cells. In these neurons, its first developmental function is to direct the epidermal cell migrations that take place during ventral enclosure of the embryo (George et al., 1998). *vab-1* and *sax-3* mutants share some epidermal abnormalities, including a partially penetrant notched head phenotype. These defects are associated with lethality that is enhanced in *sax-3; vab-1*, *sax-3;unc-6/40* and *vab-1;unc-6/40* double mutants, suggesting that SAX-3, UNC-6 and UNC-40 may also affect epidermal morphogenesis.

We show here that *vab-1* mutations disrupt the ventral guidance of amphid axons. There are three possible

explanations for this phenotype: VAB-1 and SAX-3 could mediate amphid axon guidance directly, amphid axon defects could arise indirectly as a consequence of abnormal epidermal migration, or altered interactions between neuroblasts in *vab-1* mutants could change neuronal substrata for axon migration (George et al., 1998). We favor the possibility that some effects of SAX-3 and VAB-1 are due to their actions in neurons. First, individual axons often exhibited guidance defects in *sax-3* and *vab-1* mutants even when the remainder of the nerve ring appeared normal. Second, in both *sax-3* and *vab-1* mutants, animals were observed with axon defects but no visible head morphogenesis phenotypes. Third, ventral guidance defects and anterior axon misrouting were not present in other notched-head mutants, such as *dpy-23* and *ina-1* (J. A. Z. and C. I. B., unpublished results). These results do not support a model where head morphogenesis defects account for all axon defects in *sax-3* and *vab-1* mutants.

***sax-3*, *sax-5*, *sax-9* and *vab-1* affect axon crossover at the ventral midline**

Both *sax-3/robo* and the *vab-1* Eph receptor are required to prevent aberrant axon crossing in the *C. elegans* ventral midline (Zallen et al., 1998 and the present study), along with the new genes *sax-5* and *sax-9*. Axons from the left ventral cord can travel aberrantly on the right side in the absence of left cord pioneers (Durbin, 1987). However, axons from both the left cord (HSNL) and the right cord (HSNR and *glr-1::gfp*-labeled interneurons) cross the midline inappropriately in these mutants, indicating that these defects do not merely reflect an absence of the left cord. *Drosophila* Robo has been shown to function as a receptor on axons that prevents inappropriate crossing at the midline (Kidd et al., 1998). In vertebrates and *Drosophila*, Robo proteins bind to Slit, a candidate ligand molecule that is secreted by midline cells (Brose et al., 1999; Kidd et al., 1999; Li et al., 1999), suggesting that Robo may detect a localized midline repellent.

The finding that mutations in the VAB-1/Eph receptor lead to midline crossover defects suggests the possibility that Eph receptors may participate in axon guidance at the midline. Interestingly, a transmembrane ephrin is expressed at the ventral midline of the developing neural tube in vertebrates (Bergemann et al., 1998). It is possible that the VAB-1/Eph receptor may interact with a conserved ephrin at the *C. elegans* ventral midline to prevent axons from crossing inappropriately.

***sax-1*, *sax-2*, *sax-6*, *sax-7* and *sax-8* function in nerve ring maintenance**

The genes required for nerve ring maintenance are distinct from those involved in early axon outgrowth and guidance. Five *sax* genes are specifically required for the maintenance of axon morphology during larval stages. In *sax-1* and *sax-2* mutants, neurons initiate ectopic neurites that extend late in development. Although the pathfinding of embryonic axons proceeds normally, late-growing ectopic processes wander aberrantly into the region posterior to the nerve ring. These ectopic neurites may fail to grow into the nerve ring because molecules that direct early axon guidance, such as SAX-3, are downregulated postembryonically (Zallen et al., 1998); alternatively, ectopic neurites could be indifferent to conventional guidance systems.

Posterior sensory axons are also present in mutants with

abnormal sensory activity. These include mutations in a cyclic nucleotide-gated sensory channel, mutations that affect the structure of the amphid sensory cilia, and mutations that alter ion channel function (Coburn and Bargmann, 1996; Coburn et al., 1998; Peckol et al., 1999). *sax-1* and *sax-2* might participate in an activity-dependent pathway for maintaining axon morphology, or in an alternative pathway.

The *sax-7* and *sax-8* genes identify a distinct mechanism of nerve ring maintenance. In these mutants, the nerve ring is initially correctly positioned relative to the cell bodies in first larval stage animals. However, by the second larval stage, these mutants begin to display an altered morphology, with the nerve ring increasingly posteriorly displaced relative to neuronal cell bodies. These mutants may provide information about the cell types and molecular pathways that maintain the position of the nerve ring bundle in the growing animal.

sax genes have distinct and overlapping roles in axon guidance, extension, initiation and cell migration

The diverse phenotypes of *sax* mutant animals may reflect a versatility of proteins involved in morphogenesis. Mutations in *sax-5*, *sax-9* and *unc-44* disrupt both axon guidance and extension. Similarly, netrins promote both outgrowth and guidance of vertebrate commissural axons (Kennedy et al., 1994; Serafini et al., 1994). This overlap between guidance and extension responses could occur if components of the basic cytoskeletal machinery for axon extension are targets for regulation by axon guidance pathways.

unc-44 and *unc-33* mutants exhibit ectopic neurite defects in the HSN and PDE neurons, suggesting that these genes may regulate axon initiation in multiple neuron types (this work and Hedgecock et al., 1985). UNC-44 is a *C. elegans* ankyrin, a protein that links transmembrane receptors to the actin cytoskeleton (Otsuka et al., 1995) and UNC-33-related proteins may act downstream of receptors for the semaphorin guidance cue (Goshima et al., 1995). UNC-44 is required for the proper localization of UNC-33 (W. Li and J. Shaw, personal communication); perhaps the localization of UNC-33 or other factors directs axon initiation to a single site in wild-type animals.

Mutations in the *sax-3*, *sax-5* and *sax-9* genes affect cell migration as well as axon pathfinding. All three mutations selectively disrupt the cell migration of the CAN neurons without affecting CAN axon outgrowth. A reciprocal requirement for *sax-5* and *sax-9* was observed in sensory neurons: mutations in these genes disrupted amphid axon trajectories while leaving amphid cell migrations intact. These genes may participate in axon guidance in one cellular context and cell migration in another. A parallel can be found in vertebrates, where ephrin guidance molecules direct the diverse processes of retinal axon guidance, neural crest cell migration and development of the vasculature (reviewed in Flanagan and Vanderhaeghen, 1998 and Holder and Klein, 1999).

The mechanisms by which guidance cues influence axon behavior in diverse ways are not understood, but may reflect differences in ligand presentation, receptor expression or signal transduction. The characterization of multifunctional genes required for axon growth, guidance and maintenance may provide insight into the ways guidance systems operate in distinct cellular and molecular contexts.

We thank Monica Driscoll, Ed Wu, Andy Fire and Emily Troemel for *gfp* transgenes and promoters, and Joe Hao and Erik Lundquist for identifying *ky112* as a *vab-3* allele and generating the *vab-1*; *unc-40* double mutant. We are also grateful to Tim Yu, Katja Brose, Zemer Gitai, Erin Peckol and Joe Hao for comments on the manuscript. Some strains were provided by the *Caenorhabditis* Genetics Center. This work was supported by the Howard Hughes Medical Institute and an NIH Postdoctoral Fellowship (to S. A. K.). J. A. Z. was a predoctoral fellow of the National Science Foundation and C. I. B. is an Assistant Investigator of the Howard Hughes Medical Institute.

REFERENCES

- Bargmann, C. I., Hartwig, E. and Horvitz, H. R. (1993). Odorant-selective genes and neurons mediate olfaction in *C. elegans*. *Cell* **74**, 515-527.
- Baum, P. D. and Garriga, G. (1997). Neuronal migrations and axon fasciculation are disrupted in *ina-1* integrin mutants. *Neuron* **19**, 51-62.
- Bergemann, A. D., Zhang, L., Chiang, M. K., Brambilla, R., Klein, R. and Flanagan, J. G. (1998). Ephrin-B3, a ligand for the receptor EphB3, expressed at the midline of the developing neural tube. *Oncogene* **16**, 471-480.
- Bloom, L. and Horvitz, H. R. (1997). The *Caenorhabditis elegans* gene *unc-76* and its human homologs define a new gene family involved in axonal outgrowth and fasciculation. *Proc. Natl. Acad. Sci. USA* **94**, 3414-3419.
- Brenner, S. (1974). The genetics of *Caenorhabditis elegans*. *Genetics* **77**, 71-94.
- Brose, K., Bland, K. S., Wang, K. H., Arnott, D., Henzel, W., Goodman, C. S., Tessier-Lavigne, M. and Kidd, T. (1999). Slit proteins bind Robo receptors and have an evolutionarily conserved role in repulsive axon guidance. *Cell* **96**, 795-806.
- Chalfie, M., Tu, Y., Euskirchen, G., Ward, W. W. and Prasher, D. C. (1994). Green fluorescent protein as a marker for gene expression. *Science* **263**, 802-805.
- Chan, S. S., Zheng, H., Su, M. W., Wilk, R., Killeen, M. T., Hedgecock, E. M. and Culotti, J. G. (1996). UNC-40, a *C. elegans* homolog of DCC (Deleted in Colorectal Cancer), is required in motile cells responding to UNC-6 netrin cues. *Cell* **87**, 187-195.
- Chisholm, A. D. and Horvitz, H. R. (1995). Patterning of the *Caenorhabditis elegans* head region by the Pax-6 family member *vab-3*. *Nature* **377**, 52-65.
- Coburn, C. M. and Bargmann, C. I. (1996). A putative cyclic nucleotide-gated channel is required for sensory development and function in *C. elegans*. *Neuron* **17**, 695-706.
- Coburn, C. M., Mori, I., Ohshima, Y. and Bargmann, C. I. (1998). A cyclic nucleotide-gated channel inhibits sensory axon outgrowth in larval and adult *C. elegans*: a distinct pathway for maintenance of sensory axon structure. *Development* **125**, 249-258.
- Culotti, J. G. and Merz, D. C. (1998). DCC and netrins. *Curr. Opin. Cell Biol.* **10**, 609-613.
- Desai, C., Garriga, G., McIntire, S. L. and Horvitz, H. R. (1988). A genetic pathway for the development of the *Caenorhabditis elegans* HSN motor neurons. *Nature* **336**, 638-646.
- Durbin, R. M. (1987). Studies on the development and organisation of the nervous system of *Caenorhabditis elegans*. PhD Thesis University of Cambridge, Cambridge, England.
- Flanagan, J. G. and Vanderhaeghen, P. (1998). The ephrins and Eph receptors in neural development. *Annu. Rev. Neurosci.* **21**, 309-345.
- George, S. E., Simokat, K., Hardin, J. and Chisholm, A. D. (1998). The VAB-1 Eph receptor tyrosine kinase functions in neural and epithelial morphogenesis in *C. elegans*. *Cell* **92**, 633-643.
- Goshima, Y., Nakamura, F., Strittmatter, P. and Strittmatter, S. M. (1995). Collapsin-induced growth cone collapse mediated by an intracellular protein related to UNC-33. *Nature* **376**, 509-514.
- Hamelin, M., Zhou, Y., Su, M., Scott, I. and Culotti, J. (1993). Expression of the UNC-5 guidance receptor in the touch neurons of *C. elegans* steers their axons dorsally. *Nature* **364**, 327-330.
- Hedgecock, E. M., Culotti, J. G. and Hall, D. H. (1990). The *unc-5*, *unc-6* and *unc-40* genes guide circumferential migrations of pioneer axons and mesodermal cells on the epidermis in *C. elegans*. *Neuron* **4**, 61-85.
- Hedgecock, E. M., Culotti, J. G., Thomson, J. N. and Perkins, L. A. (1985). Axonal guidance mutants of *Caenorhabditis elegans* identified by filling sensory neurons with fluorescein dyes. *Dev. Biol.* **111**, 158-70.

- Holder, N. and Klein, R.** (1999). Eph receptors and ephrins: effectors of morphogenesis. *Development* **126**, 2033-2044.
- Huang, L. S., Tzou, P. and Sternberg, P. W.** (1994). The *lin-15* locus encodes two negative regulators of *Caenorhabditis elegans* vulval development. *Mol. Biol. Cell* **5**, 395-412.
- Ishii, N., Wadsworth, W. G., Stern, B. D., Culotti, J. G. and Hedgecock, E. M.** (1992). UNC-6, a laminin-related protein, guides cell and pioneer axon migrations in *C. elegans*. *Neuron* **9**, 873-881.
- Kennedy, T. E., Serafini, T., de la Torre, J. R. and Tessier-Lavigne, M.** (1994). Netrins are diffusible chemotropic factors for commissural axons in the embryonic spinal cord. *Cell* **78**, 425-435.
- Kidd, T., Brose, K., Mitchell, K. J., Fetter, R. D., Tessier-Lavigne, M., Goodman, C. S. and Tear, G.** (1998). Roundabout controls axon crossing of the CNS midline and defines a novel subfamily of evolutionarily conserved guidance receptors. *Cell* **92**, 205-215.
- Kidd, T., Bland, K. S. and Goodman, C. S.** (1999). Slit is the midline repellent for the Robo receptor in *Drosophila*. *Cell* **96**, 785-794.
- Leung-Hagstjorn, C., Spence, A. M., Stern, B. D., Zhou, Y., Su, M. W., Hedgecock, E. M. and Culotti, J. G.** (1992). UNC-5, a transmembrane protein with immunoglobulin and thrombospondin type 1 domains, guides cell and pioneer axon migrations in *C. elegans*. *Cell* **71**, 289-299.
- Li, H., Chen, J., Wu, W., Fagali, T., Zhou, L., Yuan, W., Dupuis, S., Jiang, Z., Nash, W., Gick, C., Ornitz, D. M., Wu, J. Y. and Rao, Y.** (1999). Vertebrate Slit, a secreted ligand for the transmembrane protein Roundabout, is a repellent for olfactory bulb axons. *Cell* **96**, 807-818.
- Maricq, A. V., Peckol, E., Driscoll, M. and Bargmann, C. I.** (1995). Mechanosensory signalling in *C. elegans* mediated by the GLR-1 glutamate receptor. *Nature* **378**, 78-81.
- McIntire, S. L., Garriga, G., White, J. G., Jacobson, D. and Horvitz, H. R.** (1992). Genes necessary for directed axonal elongation or fasciculation in *Caenorhabditis elegans*. *Neuron* **8**, 307-322.
- Mello, C. and Fire, A.** (1995). DNA transformation. *Methods Cell Biol.* **48**, 451-482.
- Mueller, B. K.** (1999). Growth cone guidance: first steps towards a deeper understanding. *Annu. Rev. Neurosci.* **22**, 351-388.
- Otsuka, A. J., Franco, R., Yang, B., Shim, K. H., Tang, L. Z., Zhang, Y. Y., Boontrakulpoontawee, P., Jeyaprakash, A., Hedgecock, E., Wheaton, V. I. and Sobery, A.** (1995). An ankyrin-related gene (*unc-44*) is necessary for proper axonal guidance in *Caenorhabditis elegans*. *J. Cell Biol.* **129**, 1081-1092.
- Peckol, E. L., Zallen, J. A., Yarrow, J. C. and Bargmann, C. I.** (1999). Sensory activity affects sensory axon development in *C. elegans*. *Development* **126**, 1891-1902.
- Riddle, D. L., Swanson, M. M. and Albert, P. S.** (1981). Interacting genes in nematode dauer larva formation. *Nature* **290**, 668-671.
- Schackwitz, W. S., Inoue, T. and Thomas, J. H.** (1996). Chemosensory neurons function in parallel to mediate a pheromone response in *C. elegans*. *Neuron* **17**, 719-728.
- Serafini, T., Kennedy, T. E., Galko, M. J., Mirzayan, C., Jessell, T. M. and Tessier-Lavigne, M.** (1994). The netrins define a family of axon outgrowth-promoting proteins homologous to *C. elegans* UNC-6. *Cell* **78**, 409-424.
- Siddiqui, S. S.** (1990). Mutations affecting axonal outgrowth and guidance of motor neurons and mechanosensory neurons in the nematode *Caenorhabditis elegans*. *Neurosci. Res. (Suppl.)* **13**, 171-190.
- Siddiqui, S. S. and Culotti, J. G.** (1991). Examination of neurons in wild type and mutants of *Caenorhabditis elegans* using antibodies to horseradish peroxidase. *J. Neurogenet.* **7**, 193-211.
- Sulston, J. E., Schierenberg, E., White, J. G. and Thomson, J. N.** (1983). The embryonic cell lineage of the nematode *Caenorhabditis elegans*. *Dev. Biol.* **100**, 64-119.
- Tessier-Lavigne, M. and Goodman, C. S.** (1996). The molecular biology of axon guidance. *Science* **274**, 1123-1133.
- Vowels, J. J. and Thomas, J. H.** (1992). Genetic analysis of chemosensory control of dauer formation in *Caenorhabditis elegans*. *Genetics* **130**, 105-123.
- Wadsworth, W. G., Bhatt, H. and Hedgecock, E. M.** (1996). Neuroglia and pioneer neurons express UNC-6 to provide global and local netrin cues for guiding migrations in *C. elegans*. *Neuron* **16**, 35-46.
- Wang, B. B., Muller-Immergluck, M. M., Austin, J., Robinson, N. T., Chisholm, A. and Kenyon, C.** (1993). A homeotic gene cluster patterns the anteroposterior body axis of *C. elegans*. *Cell* **74**, 29-42.
- White, J. G., Southgate, E., Thomson, J. N. and Brenner, S.** (1976). The structure of the ventral nerve cord of *Caenorhabditis elegans*. *Phil. Transact. R. Soc. Lond. B* **275**, 327-348.
- White, J. G., Southgate, E., Thomson, J. N. and Brenner, S.** (1986). The structure of the nervous system of the nematode *Caenorhabditis elegans*. *Phil. Transact. R. Soc. Lond. B* **314**, 1-340.
- Zallen, J. A., Yi, B. A. and Bargmann, C. I.** (1998). The conserved immunoglobulin superfamily member SAX-3/Robo directs multiple aspects of axon guidance in *C. elegans*. *Cell* **92**, 217-227.